ELSEVIER

Journal of Alloys and Compounds 408–412 (2006) 701–705

Journal of ALLOYS AND COMPOUNDS

www.elsevier.com/locate/jallcom

Preparation and evaluation of the rare earth doped nanoparticle SiO_2–PVP hybrid thin film by sol–gel method

H. Nakajima, K. Kawano *

Department of Electronic Engineering, The University of Electro-Communications, Chofugaoka, 1-5-1 Chofu, Tokyo 182-8585, Japan

Received 2 August 2004; received in revised form 17 December 2004; accepted 13 January 2005
Available online 1 July 2005

Abstract

For the purpose of development of high-luminosity and high-scattering photoluminescence materials, we studied preparation and evaluation of the thin films of firstly SiO_2 nanoparticles with the particle size of 10–30 nm and next, SiO_2–PVP inorganic–organic hybrid ones with the sizes 100–150 nm, both doped with the rare earth (RE) Eu ions by the sol–gel method. Application of the former nanoparticles is expected to increase light scattering effect. For the hybrid film, the starting sol was C_2H_5OH solutions of silicon-alkoxide $Si(OC_2H_5)_4$ doped with $Eu(fod)_3$ complexes and polymer resin PVP, in which NH_4OH was used for promoting hydroxis. The FE-SEM observation for the obtained film surface revealed formations of homogeneously high-density nanoparticle SiO_2 spheres with the sizes 100–150 nm. The SiO_2–PVP hybrid thin film exhibited higher PL and PLE by 50% than only PVP thin film. The PL spectra showed mainly sharp lines with the peaks of 580, 592 and 614 nm, and were assigned to the f–f transitions of $Eu^{3+}(4f^6)$ through thermal transfer from the excited singlet and triplet states for $Eu(fod)_3$ complexes.

Keywords: Nanoparticle; SiO_2; PVP; Hybrid thin film; Eu; Sol–gel method

1. Introduction

It is well known that the rare earth (RE) ions such as Eu, Sm and Tb exhibit a high yield of luminescence in the visible light region [1]. In recent years, research and development of the luminescent materials using these rare earth ions have attracted attention of a lot of optodevice engineers. The rare earth ions can transform the absorption energy in shorter wavelength region into the luminescence energy in the longer wavelength region with high-luminosity. If this wavelength conversion is applied to solar cells, the cells can produce larger electric power than current solar cells in use because they usually have spectroscopic sensitivity peaks at longer wavelengths as compared with the solar light distribution [2]. For the purpose of development of a precursor doped with RE ions to improve the conversion efficiency of solar cell, we have so far proceeded to fabricate and evaluate various crystals and thin film doped with the rare earth ions [3].

In the present study, we attempted to apply the rare earth doped nanoparticle SiO_2 and SiO_2–PVP inorganic–organic hybrid nanoparticles because we can expect the nanoparticles to obtain high-luminosity by their multiple scatterings, besides the normal luminescence and transmitted light. At first, the mechanism of multiple scattering by nanoparticles is explained in comparison with the case of normal bulk. Next, the actual fabrication process of thin film phosphor involving rare earth ions is described. Moreover, the optical measurements such as transmission, luminescence and excitation are performed with their dependencies for RE concentrations and annealing temperatures. Finally, the evaluation of obtained films are made through discussion to practical application.

* Corresponding author. Tel.: +81 424 43 5144.
E-mail address: kawano@ee.uec.ac.jp (K. Kawano).

0925-8388/$ – see front matter © 2005 Elsevier B.V. All rights reserved.
doi:10.1016/j.jallcom.2005.01.076

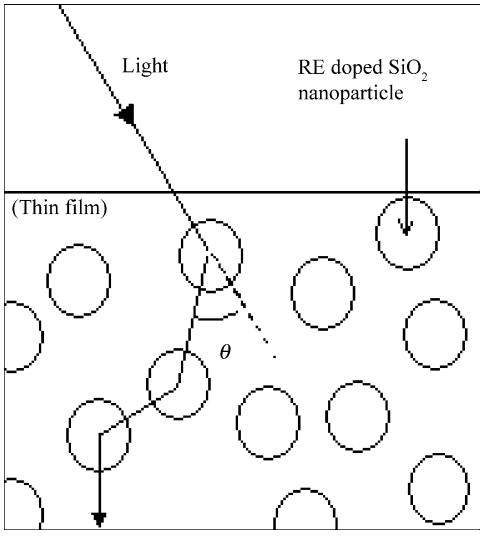

Fig. 1. Schematic figure of light scatterings by nanoparticles.

2. Rayleigh multiple scattering by nanoparticles

The most important difference [4,5] between the present RE doped nanoparticle system and the normal bulk system rests on light scattering. For the nanoparticle (particle size, ρ) system, the scattering phenomenon for solar light (wavelength, λ) is governed under the condition $\rho \ll \lambda$ by Rayleigh scattering whose intensity is proportional to the converse of 4th power of wavelength. Actually, the simulation results considering the scattering angle of $\pi/2$ at the wavelength of 300 nm indicated the exponential increase of the scattering intensities for the particle sizes less than 30 nm.

Moreover, for the nanoparticle system, the scattering effects must be carried out in a multiple feature. The schematic figure of light multi-scattering by nanoparticles is shown in Fig. 1.

The incident light enters into the first particle and scatters with the angle θ and in succession, from the nth to $(n+1)$th, the scatterings continue infinitely. These multiple scattering schemes are described along correspondence to the analyses of the dynamical theory of diffraction for X-ray diffraction [6].

The electric field waves $\boldsymbol{E}_\mathrm{i}$, $\boldsymbol{E}_\mathrm{s}$ of the incident light and the scattering light are given with their amplitudes, according to the normal notations, as follows [7]:

$$\left.\begin{aligned} \boldsymbol{E}_\mathrm{i} &= \boldsymbol{E}_\mathrm{oi} \exp\, \mathrm{i}(\omega_\mathrm{i} t - \boldsymbol{k}_\mathrm{i}\boldsymbol{r}) \\ \boldsymbol{E}_\mathrm{s} &= \boldsymbol{E}_\mathrm{os} \exp\, \mathrm{i}(\omega_\mathrm{s} t - \boldsymbol{k}_\mathrm{s}\boldsymbol{r}) \end{aligned}\right\} \quad (1)$$

Then, putting the transmission rate as γ and the scattering rate as s, the following recursion formula hold:

$$\left.\begin{aligned} E_{\mathrm{s},n} &= sE_{\mathrm{i},n} + \gamma E_{\mathrm{s}(n+1)} \exp(-\mathrm{i}\boldsymbol{kd}) \\ E_{\mathrm{i},n} &= \gamma E_{\mathrm{i},(n-1)} \exp(-\mathrm{i}\boldsymbol{kd}) + sE_{\mathrm{s},n} \exp(-2\mathrm{i}\boldsymbol{kd}) \end{aligned}\right\} \quad (2)$$

and for the first scattering, the relationship is expressed as follows:

$$E_{\mathrm{s,o}} = sE_{\mathrm{i,o}} + \gamma E_{\mathrm{s},1} \exp(-\mathrm{i}\boldsymbol{kd}), \quad (3)$$

where $\boldsymbol{d}$ is the mean distance vector among particles. When the particle size was put ρ, the intensity $|E_\mathrm{s}|^2$ of the total scattering light was calculated and the following relation holds [5]:

$$|E_\mathrm{s}|^2 = \frac{\pi^2}{2}(1+\cos^2\theta)\frac{N|\alpha|^2}{{\varepsilon_0}^2\rho^3\lambda^4}|E_0|^2, \quad (4)$$

where α is the polarizability of SiO_2, ε_0 the dielectric constant of vacuum and N is the particle density equal to the converse of 3rd power of d. This means that the scattering light increases proportional to the converse of 3rd power of ρ, adding to the converse of 4th power of wavelength. So, the scattering light intensities are enhanced in the shorter wavelength region and the smaller particle sizes. The RE earth ion will absorb this blue scattering light and emit as its luminescence to the longer wavelength, adding the original luminescence.

3. Experiments

3.1. SiO_2 nanoparticles with Eu

The solution of SiO_2 ultra-fine particles was supplied from Seishin Co. This solution involves SiO_2 nanoparticles with 10–30 nm diameter. The fabrication of nanoparticles SiO_2:Eu thin film phosphor by sol–gel method process is shown in Fig. 2 [8–10].

First of all, $EuCl_3$ is dissolved into C_2H_5OH with the concentration of 0.5 mol/L and its solvent is mixed with 0.5 wt% SiO_2 solution with various volume ratios, in which H_3BO_3 is added into the solution to hold uniformity and

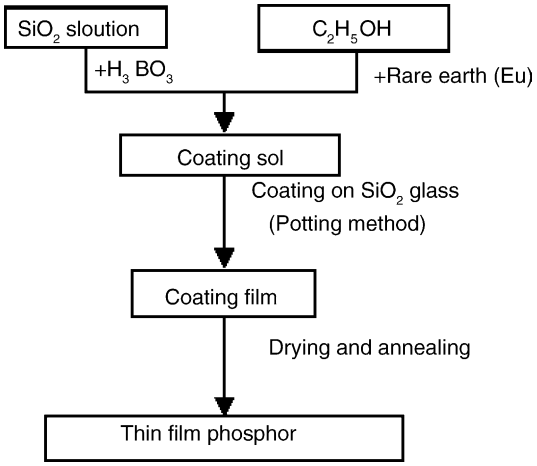

Fig. 2. Fabrication process of the nanoparticle SiO_2:Eu thin film phosphor by sol–gel method.

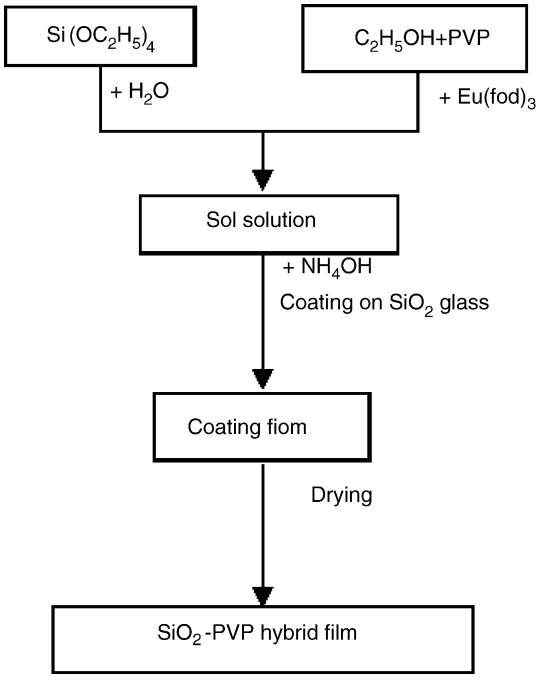

Fig. 3. Fabrication process of the SiO_2–PVP hybrid nanoparticles thin film phosphor with Eu by sol–gel method.

to protect deposition and phase separation. Thus, obtained solvents or sol is coated on the substrate with size of 1 mm × 10 mm × 40 mm by the potting method that the sol is dropped on the substrate to be immediately stood up right for formation of homogeneous film. After the coating, film was dried for several hours to 1 day at room temperature, it was annealed for 15 min at 300–500 °C in nitrogen gas atmosphere with the oxidation–deoxidation furnace (Asahi Science Co., ARF-153W).

3.2. SiO_2–PVP hybrid nanoparticles with Eu

The starting sol was C_2H_5OH solutions of silicon-alkoxide $Si(OC_2H_5)_4$ doped with $Eu(fod)_3$ complexes and polymer resin PVP, in which NH_4OH was used for promoting hydroxis. The gel was obtained by drying the sol solutions on fuzed quartz substrates for a few days in air atmosphere. The fabrication process of the SiO_2–PVP hybrid nanoparticles thin film phosphor with Eu by sol–gel method is shown in Fig. 3.

Evaluations of fabricated thin film phosphor were carried out by optical analysis measurements; transmission, luminescence and excitation. Transmission spectrum was measured to investigate the influence of light scattering of nanoparticles with a double-beam spectrophotometer (Shimazu Co., UV-200). Luminescence and excitation spectra were measured using a spectrofluorometer (JASCO, FP-6500). The direct observation of formed nanoparticles was performed by FE-SEM (JEOL, JSM-6340F).

4. Results and discussion

4.1. SiO_2 nanoparticles with Eu

The transmission spectra of the coating thin films on SiO_2 glass substrates were compared with that of only the SiO_2 glass in the wavelength region from 220 to 800 nm [11]. The transmittances of the films have decreased from 57 to 22% much lower in shorter wavelength, in which the SiO_2 glass was 95% in all the region. The remarkable decrease in all the wavelength suggests the unsuitabilities of either the mixture ratio of the coating sol or the annealing temperature. The decrease in short wavelengths mean the existence of absorption bands, possibly the influence of RE absorption for Rayleigh scattering of nanoparticles because it was confirmed by the excitation spectra mentioned later.

Fig. 4(a and b) show the luminescence spectrum for the excited wavelength of 253 nm and the excitation spectrum for the emission of 614 nm, respectively, for the thin film with Eu concentration of 0.17 mol/L and the annealing temperature of 300 °C. The characteristics of luminescence exhibit a broad band around the peak of 470 nm, a little broad band with the peak of 579 nm and the sharp lines with the peaks of 590 and 614 nm. Since the broad band has appeared also for SiO_2 glass, it is determined to be responsible for the glass substrate. The other lines were assigned to be caused by the energy separations of f–f transitions of $Eu^{3+}(4f^6)$ from the energy level diagrams, as shown in Fig. 5, in which $^5D_0 \rightarrow {}^7F_J$ ($J = 0,1$ and 2) transitions were $^5D_0 \rightarrow {}^7F_0$ (579 nm), $^5D_0 \rightarrow {}^7F_1$ (590 nm) and $^5D_0 \rightarrow {}^7F_2$ (614 nm), respectively.

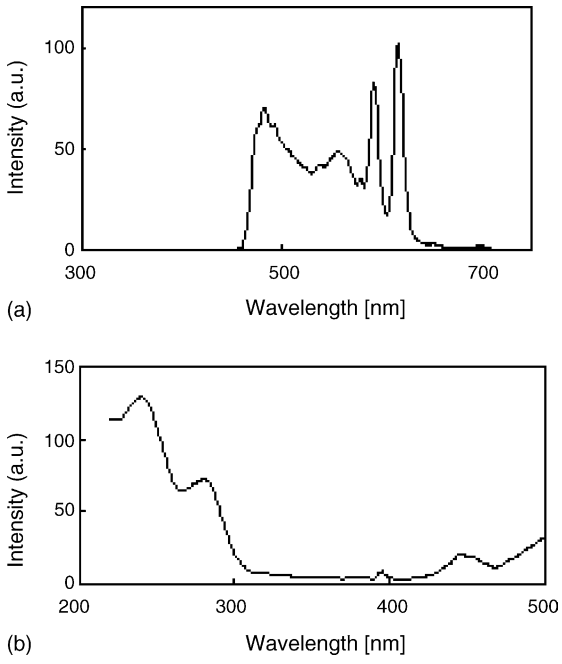

Fig. 4. For the sample with Eu of the concentration of 0.17 mol/L: (a) luminescence spectrum for 253 nm excitation and (b) excitation spectrum for 614 nm luminescence.

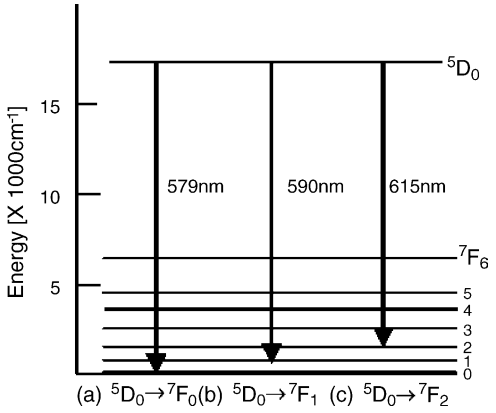

Fig. 5. Assignments of observed sharp lines of: (a) 579 nm, (b) 590 nm and (c) 615 nm in $^5D_0 \rightarrow {}^7F_J$ transitions of the energy level diagram for Eu^{3+} ion.

On the other hand, the excitation spectrum exhibited the two broad bands with peaks of 230 and 280 nm bands in deep UV region and the other weak bands of 390 nm ($^7F_0 \rightarrow {}^5D_3$) and 440 nm ($^7F_0 \rightarrow {}^5D_2$), as shown in Fig. 4(b). The fairly deep UV two bands originate presumably from the charge transfer band of Eu^{3+} to the ground $^7F_0$ and $^7F_1$ states [1]. Note here that the base enhancements below 300 nm may be due to the influence of the scattering of nanoparticles mentioned in Section 2.

About especially intense lines of 590 and 614 nm, we measured the dependencies of luminescence intensities against the annealing temperatures and the Eu concentrations. The results are shown in Fig. 6(a and b), respectively. Their intensities both increased through the treatment of annealings, but indicated the maximums around 350 °C. As to the concentration dependencies at an annealing temperature 300 °C, also both their intensities decreased monotonously for the increase of concentrations. For getting more intensities, fabrications of the films with less concentration were tried, but failed to have gel state grown during sol mixings owing to excess SiO_2 solution [12].

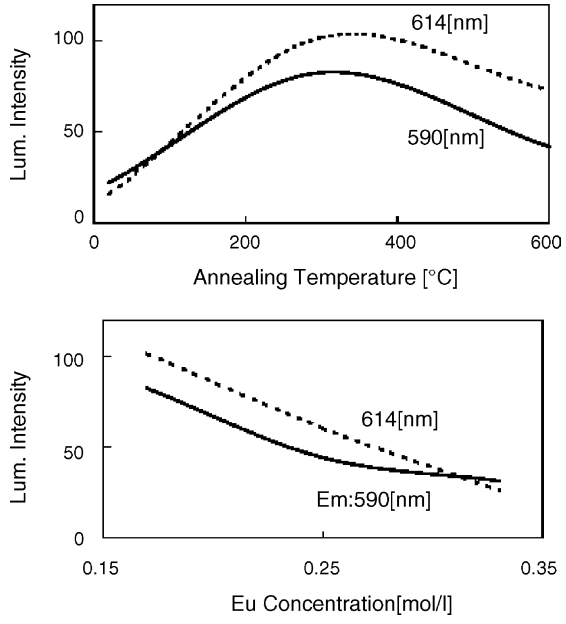

Fig. 6. Variations of luminescence intensities against: (a) the annealing temperature and (b) the Eu concentration under 300 °C annealing for the sharp lines of 590 and 614 nm.

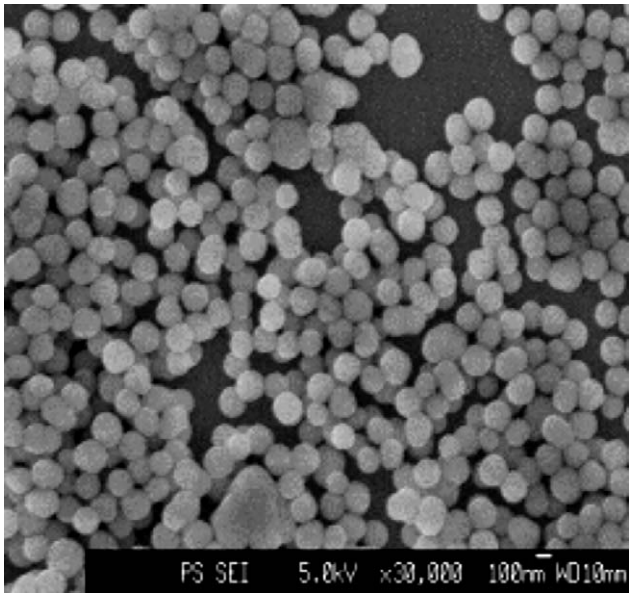

Fig. 7. FE-SEM photograph for SiO_2 with $Eu(fod)_3$.

4.2. SiO_2–PVP hybrid nanoparticles with Eu

The FE-SEM observation of obtained film surface revealed formations of homogeneously high-density nanoparticle SiO_2 spheres with the size 100–150 nm, as shown in Fig. 7.

The PL spectra showed three sharp lines with the peaks of 580, 592 and 614 nm, as shown in Fig. 8, and were assigned to the f–f transitions of $Eu^{3+}(4f^6)$ through thermal transfer from the excited singlet and triplet states for $Eu(fod)_3$ complexes.

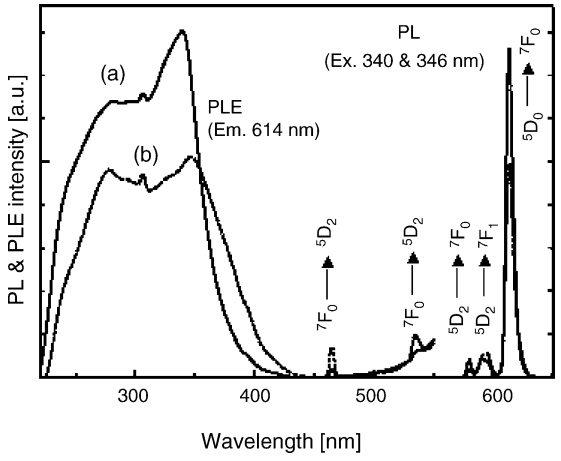

Fig. 8. PL and PLE spectra of $Eu(fod)_3$ doped with: (a) SiO_2–PVP hybrid thin film and (b) PVP thin film.

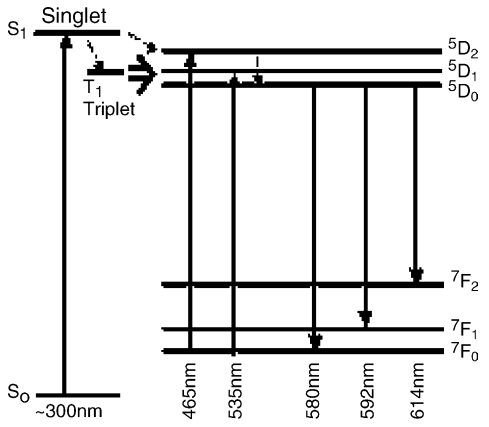

Fig. 9. The mechanism of luminescence in $Eu(fod)_3$ complexes.

We can notice that the SiO_2–PVP hybrid thin film with Eu exhibited higher PL and PLE by 50% than a simple PVP thin film with Eu. This evidence suggests that the hybridizations of inorganic SiO_2 and organic PVP are very effective to obtain higher PL and PLE intensities. Moreover, the increase of porosity of the hybrid film by annealed PVP may assist to enhance the nanosize effect [13–15].

The mechanism of luminescence of the SiO_2–PVP hybrid system is indicated in Fig. 9. At first, the absorption of about 300 nm from the ground state S_0 to the excited singlet state S_1 in $Eu(fod)_3$ complexes occurs and, in part, falls to the excited triplet state T_1 through the cross relaxation, partly, to $^5D_2$ state in the $Eu^{3+}(4f^6)$ state. The energy transfer from T_1 to the excited states of Eu^{3+} is thermally carried out. On the other hand, the intratransition in Eu^{3+} itself, the two absorptions of $^7F_0$ to $^5D_2$ (465 nm) and $^7F_0$ to $^5D_1$ (535 nm) and the same three emission lines of 580, 592 and 614 nm that in Fig. 5 are observed.

5. Conclusions

We studied the preparations and the evaluations of the thin films of firstly SiO_2 nanoparticles with the particle size of 10–30 nm and next, SiO_2–PVP inorganic–organic hybrid ones with the size 100–150 nm, both doped with the rare earth Eu ions by the sol–gel method. The obtained results are summarized as follows:

(i) The luminescence spectra showed three sharp lines of the f–f transitions of $Eu^{3+}(4f^6)$ in SiO_2 nanoparticles.

(ii) For the SiO_2 nanoparticles with Eu, the annealing temperature dependencies of observed peak intensities exhibited the maximums around 350 °C.

(iii) The SiO_2–PVP hybrid thin film exhibited higher PL and PLE by 50% than only PVP thin film. The effectiveness of the inorganic and organic hybridization was confirmed.

(iv) All the observed PL spectra are available for improvement of Si-solar cell efficiency.

Acknowledgment

We thank sincerely H. Tanaka, Seishin Co. for offering SiO_2 ultra-fine particle solutions.

References

[1] G. Adachi, Science of Rare-Earth, Kagaku-Dojin Publication, 1999, pp. 127–163 (in Japanese).
[2] B.C. Hong, K. Kawano, Sol. Energy Mater. Sol. Cells 64 (2003) 447.
[3] R. Nakata, K. Kawano, Application of rare earth complexes for photovoltaic precursors, in: G. Adachi (Ed.), Report of a Priority Area Research Program "New Development of Studies on Rare Earth Complexes", supported by The Ministry of Education, Science, Sports and Culture, 1997, pp. 871–876.
[4] N. Ichinose, Y. Ozeki, S. Kashu, Introduction of Ultra-Fine Particle Technology, Ohm Co., 1988 (Chapter 1) (in Japanese).
[5] K. Kawamura, Ultra-Fine Particle, Maruzen, 1987 (Chapter 1) (in Japanese).
[6] S. Miyake, X-ray Diffraction, Asakura Publication, 1969 (Chapter 5) (in Japanese).
[7] K. Kudo, Fundamentals of Optophysical Properties, Ohm Publication, 1977 (Chapter 8) (in Japanese).
[8] Japan Materials Science Society, An Ultra-Fine Particle and Material, Syokabo Publication, 1993, pp. 1–32 (in Japanese).
[9] S. Sakka, Science of Sol–Gel Process, Agune Publication, 1988, pp. 85–103 (in Japanese).
[10] S. Sakka, Application of a Sol–Gel Process, Agune Publication, 1997, pp. 116–128 (in Japanese).
[11] W. Kaijo, Master Thesis. UEC (March 2002) (in Japanese).
[12] H. Nakajima, W. Kaijo, K. Kawano, Proc. Int. Works Mod. Sci. Tech. (IWMST), Tokyo (2002) 66.
[13] H. Kozuka, M. Kajimura, Chem. Lett. 28 (1999) 1029–1030.
[14] H. Kozuka, M. Kajimura, T. Hirano, K. Katayama, J. Sol–Gel Sci. Technol. 19 (2000) 205–209.
[15] H. Kozuka, M. Kajimura, J. Am. Ceram. Soc. 83 (2000) 1056–1062.